Automatic Generation Control of Three Area Hybrid Power System by Sine Cosine Optimized Dual Mode, Fractional Order Controller

A.P. Srivishnupriya*‡, M. Mohamed Thameem Ansari**, N.J. Vinoth Kumar***

**Department of Electrical Engineering, Faculty of Engineering and Technology, Annamalai University, Annamalai Nagar, Tamilnadu, India-608002.

** Department of Electrical Engineering, Faculty of Engineering and Technology, Annamalai University, Annamalai Nagar, Tamilnadu, India-608002.

*** Department of Electrical and Electronics Engineering Government Polytechnic College, Nagercoil, Tamilnadu, India- 629004

(vishnuap28@gmail.com, ansariaueee@gmail.com, vinothkumarnj@gmail.com)

‡ Corresponding Author; A.P. Srivishnupriya, Postal address, Tel: +91 9442179013, vishnuap28@gmail.com

Received: 01.06.2022 Accepted: 30.07.2022

Abstract - Around the world, a radical change in power generation technology is taking place. As a result, traditional energy sources are being transformed with reliable renewable energy sources and Distributed Generation sources. Combining these different generations improves the system's efficiency, but frequency fluctuation will be more frequent than in the traditional system due to their volatile generation. In this article, an efficient and simple dual-mode fractional order controller (SDMFOPI) tuned using a sine cosine optimization algorithm is proposed and tested in three area hybrid power system (TAHPS) with superconducting magnetic energy storage to subdue the frequency fluctuation problem. The proposed SDMFOPI controller is more robust as it provides more space for tuning the parameters of the controller. To manifest its potency, it is furthermore compared with various controllers such as conventional Proportional integral controller, sine cosine algorithm tuned fractional proportional-integral controller, and SCO algorithm tuned dual-mode proportional-integral controller. Moreover, different case studies were carried out along with sensitivity analysis for the TAHPS. From the obtained result, it is evident that the proposed controller is more efficient and fit for the frequency regulation of the TAHPS.

Keywords Load frequency control, Superconducting magnetic energy storage, Dual-mode scheme, Sine cosine Optimization Algorithm, Three-area hybrid power system.

NOTATION	
LFC	Load frequency control
SCOA	Sine cosine Optimization Algorithm
HPS	Hybrid Power System
TAHPS	Three-area hybrid power system
ACE	Area control error
ISE	Integral square error
SMES	Superconducting Magnetic Energy Storage
SLP	Step load perturbation
X_n^i	Current solution

P_{ti}	Best solutions 'position
$\Delta G_{T,}$ $\Delta G_{H,}$ $\Delta G_{W,}$ $\Delta G_{P,}$ $\Delta G_{T,}$ $\Delta G_{H,}$ $\Delta G_{W,}$ ΔG_{D}	Change in power generated in thermal, hydro, wind, solar, and diesel plant for a small change in step load perturbation
ΔG_{HVDC}	Change in power in HVDC line due to small change in step load perturbation.
ΔG_{SMESI}	Change in power in SMESs due to small change in step load perturbation.
E	Switching limit
SFOPI	SCO-based fractional-order proportional-integral controller.
SDMFOPI	SCO-based dual mode fractional order, proportional-integral controller.
SDMPI	SCO-based dual-mode proportional-integral controller.
r1, r2, r3, r4	Random numbers
U(t)	controller output
E(t)	error signal
ΔFj	frequency change in the jth area
$\Delta P_{tie\text{-}linej}$	Tieline power in j^{th} area
U(t)	controller output
E(t)	error signal
λ_i	fractional operator
Ki, Kp	Integral gain and proportional gain
B1, B2	Biasing coefficient in area 1 area 2

1. Introduction

Recently our conventional power system is facing many issues in various aspects of fossil fuel depletion, escalation of load connected, a rise of electricity prize, aging of traditional power plants, etc. This leads to modification in the traditional system. Distributed generation (DG) refers to the small power plants, which comprise both alternative and renewable energy sources. The small hydro plants, diesel engine generators, Wind Turbines System (WTS), Fuel Cells (FC), micro-turbines, photovoltaic (PV) systems, reciprocating engines, etc., and storage technologies such as battery energy storage systems, flywheels, ultra-capacitors, and SMES. The traditional system which includes various distributed generations and storage systems forms a hybrid power system (HPS). The HPS has sundry benefits such as fuel diversification, very less expel of greenhouse gases, low maintenance, less power cost, availability in abundance, etc., and assures continuous, stable, efficient, low-cost power to the users, with less emission of greenhouse gases. Different types of HPS are discussed in the following works. Firstly, a hybrid WTS-Diesel plant and Static Synchronous Compensator and SMES are studied in [1] and [2]. Whereas in [3] authors work with HPS with wind power and thermal power and in [4], isolated HPS of WTS-Biomass is designed and simulated. It is observed that different combinations of generations lead to different types of HPS like solar PV-FC-Battery, PV-WTS, WTS-Battery-solar PV, thermal -wind-hydropower, and systems with electrical vehicles also studied [5]– [9]. In the above-discussed HPSs, Frequency Deviation (FD) is inevitable, it is more prominent due to the presence of dynamic generation sources. LFC can overcome FD due to the power mismatch between the connected generation and load caused by a sudden change in either case by tracking system frequency and tie-line power, calculating the net change in necessary power generation, and adjusting the specific position of generators in all the area to keep power generation and load demand in balance. Adding the energy storage devices along with renewable energy sources may reduce the risk of frequency deviation problems in HPS.[10]. Also, different types of control approaches have been developed up to now and categorized into four major methods namely classical, modern, intelligent and soft computing-based techniques [11]. The classical proportional-integral-derivative (PID) is the most extensively used controller for power system control, which is more significant. Recently, authors in [12] designed a PID controller for LFC by considering communication delay. Likewise, for HPS with UC and UPFC frequency control is done using a PID controller [13]. And also, in [14], A Ziegler–Nichols- PID controller is used for automated generation control of both conventional and PV integrated power systems. In the PID controller, the integral controller's response is delayed during the transient period. On the other side, it is also worth noting that cascading many controllers and techniques may produce better results [15-17]. But incorporating different controllers and techniques is a complicated one. Also, the application of intelligent approaches based on human understanding, such as fuzzy logic, appears to be able to increase performance, overcome model uncertainties and minimize costs [18]. But, due to the reason that those fuzzy systems rely on erroneous inputs and data, their accuracy is jeopardized. There is no one-size-fits-all strategy for applying Fuzzy Logic to address an issue. As a result, several solutions to a single problem emerge, causing misunderstanding. As highlighted by the literature survey, the difficulty is to overcome complex controller structure as well as uncertainty and inaccuracy. The above-

mentioned problems can be overpowered by effectuating the dual-mode fractional-order proportional-integral controller (DMFOPI). This dual-mode control has no complicated structure and is simple to apply. Also, recent research has found that FOPI controllers outperform conventional PID controllers by providing superior results. High-performance optimizing algorithms are always appropriate in a controller for load frequency management [19-21]. Thereby for the proposed method, an SCO algorithm tuned dual-mode fractional-order proportional-integral controller (SDMFOPI) is employed for the load frequency problem. In a Three Area Hybrid Power System (TAHPS) the proposed control mechanism is used for the load frequency problem. The following is the organization of the upcoming work. The proposed work's aims are discussed in section 2, TAHPS is explained in section 3, and the mathematical modeling of the system is presented in section 4. The proposed SDMFOPI controller and other controllers are discussed in Section 5, while the SCO algorithm is explained in Section 6. Finally, Section 7 gives the simulation results of the suggested work with several cases and discussion, followed by a conclusion in Section 8.

2. Figures And Tables Objectives of The Research Work

- The major goals of the research work are categorized below.
- To design a robust SDMFOPI controller which is more suitable for LFC of TAHPS.
- To obtain the optimized gains of the SDMFOPI controller using a simple, robust SCO algorithm.
- To model a TAHPS to test the proposed SDMFOPI controller.
- To do the comparison with other types of controllers to prove its reliability among other controllers.
- To discuss different scenarios for TAHPS with the SDMFOPI controller, to prove its effectiveness.

3. Test system examined

In this paper, an interconnected TAHPS is investigated for verifying the controller characteristics. Herein, each area is a combination of two-generation sources and a SMES system. The TAHPS system considered here depicts the conversion of a conventional power system to a modern system as each area is a combination of traditional and renewable energy sources (RES) and SMES [22-23]. Renewable energy integration has more benefits [24-25]. Out of three areas, area1 is a combination of thermal, wind, and SMES 1 then area 2 is a combination of hydro, diesel, and SMES 2 at last area3 is a combination of thermal, PV, and SMES 3. Likewise, all the three areas are interconnected to form a TAHPS as shown in Fig 1.

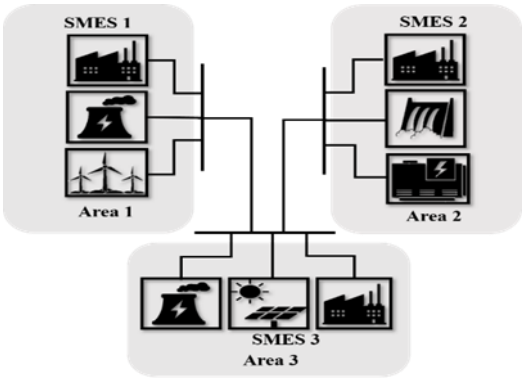

Fig. 1. Three area hybrid system one-line diagram

4. Mathematical Modeling of The Generation Units

The modeling approach aids in identifying and understanding the components and helps in making decisions regarding the selection of components. The mathematical model of the various generation sources and SMESs in the TAHPS for a small change in load is presented in the following equations from equations (1)-(11).

- Thermal power plant

$$\Delta G_{T1}=K_{T1}/T_{T1}s+1 \quad (1)$$

$$\Delta G_{T2}= K_{T2}\ T_{T2}\ s+1/\ T_{T2}s+1 \quad (2)$$

$$\Delta G_{T3}= K_{T3}/\ T_{T3}s+1 \quad (3)$$

In equations (1) to (3) K_{T1}, K_{T2}, K_{T3} represent the gain constants and of the governor, reheater, and turbine of the thermal plant, and T_{T1}, T_{T2}, T_{T3} are their corresponding time constants.

$$\Delta G_{PS}=K_{PS}/T_{PS}s+1 \quad (4)$$

Were, K_{PS} is the gain constant and T_{PS} is the time constant of the power system.

- Hydropower plant

$$\Delta G_{H1}=(K_{H1}/T_{H1}s+1)\ *(T_{H11}s+1/T_{H12}s+1) \quad (5)$$

$$\Delta G_{H2}= (\text{—}\ T_{H2}s+1/0.5*T_{H2}s+1) \quad (6)$$

In equations (5) and (6), K_{H1} and T_{H1} are the hydro governor gain and time constant. Whereas T_{H11} and T_{H12} are rise time, transient droop, and nominal flow time of the hydro governor.

- Solar PV Plant:

$$\Delta G_{P1}= (K_{P1}+K_{P2}/(s^2+T_{P1}s+T_{p2})) \quad (7)$$

In (7), solar PV plant $K_{P1}$and K_{P2} are the gain, and T_{P1} and T_{P2} are their related time constants.

- Wind power plant:

Wind turbines can produce electricity more efficiently at varied speeds, depending with the variance in wind speed[26].In (8) K_{w1}, K_{w2} and K_{w3} are the wind power gains and T_{w1} and T_{w2} are their related time constants.

$$\Delta G_{W1}=((K_{W1}*K_{W2}*(1+T_{W1}s))/(1+T_{W2})*(1+2s+s^2))) \quad (8)$$

$$\Delta G_{W2} =K_{W3}/1+s \quad (9)$$

- SMES (Superconducting Magnetic Energy Storage) system:

The SMES is the ideal system for storing a huge quantity of energy in the form of a magnetic field using a supercooled coil while also releasing a significant amount of power in a fraction of a cycle. These serve as backup devices and are usually used to keep the electrical system's power balance when the generation exceeds the demand Stored energy is released to the grid.

$$\Delta P_{SMESi}= (1+sT_{i1}/1+sT_{i3})*(1+sT_{i2}/1+sT_{i4})*(K_{SMESS}/1+sT_{SMESS}) \quad (10)$$

Where Ti1, T_{i2}, T_{i3}, T_{i4}, and T_{SMESS} are the time constants and K_{SMESS} denotes the stabilization gain of ith SMES.

- HVDC (High Voltage Direct Current) system:

The HVDC systems' primary use is to improve the regulation of power flow in AC grids, either to carry power between two distant places or to assist the AC system. To increase the tie-line power transfer capability, HVDC lines can be added in tandem with the AC lines. The relevant switching strategy controls the operation of the converter-inverter portion that is incorporated into the HVDC line. A first-order transfer function was used to model the HVDC line.

$$\Delta P_{HVDC}= K_{DC}/ (1+T_{DC}) \quad (11)$$

5. Design of Proposed SMFOPI Controller and Other Controllers

This chapter discusses the design of the proposed SDMFOPI controller as well as the design of other controllers.

5.1. Design of Conventional PI Controller

A PI controller is a form of controller that is widely employed to solve the LFC problem. One of the most common approaches for calibrating the PI controller is trial and error. The gain value of the proportional controller is computed first in this technique, with the integral gain set to zero. An integral gain value is found using the proportionate gain value. It is a fixed-gain type that may or may not be successful in all situations. The output equation (12) is as follows. The ISE criterion is used as the performance index in tuning gains.

$$U(t) = K_p E(t) + \int_0^t \frac{K_i}{s} E(t) \quad (12)$$

5.2. Design of SFOPI Controller

According to a recent study, fractional-order controllers may perform better than integer-order controllers in terms of robustness and system performance. Its uses are being investigated, and new tuning methods are being developed [27-28]. These controllers employ fractional calculus to calculate their descent. The transfer function of the FOPI controller is defined in equation (13) where λ is the fractional operator for the integral controller. Here the FOPI controller's gains are optimized by the SCO algorithm, therefore the term SFOPI is used.

$$U(t) = K_p E(t) + \int_0^t \frac{K_i}{s^\lambda} E(t) \quad (13)$$

5.3. Design of SDMPI Controller

The PI controller's reaction is more oscillatory with fixed gains. This issue can be resolved by utilizing the dual-mode approach in the PI controller [29-30]. The dual mode scheme is explained as follows. Depending on the error change, the controller's configuration alters. Due to their speedier transient response, proportional controllers are employed to reach steady state conditions significantly more quickly. When the rate of error change E(t) is sufficiently large, the proportional controller will operate during the transient period. When the rate of error change E(t)is modest, the integral controller would be a good choice. The dual scheme for the PI controller is thus implemented in the SDMPI and SDMFOPI controller. From the Eqn (14) and (15), U(t) is the control signal fired out from the controller whereas E(t) is the error signal which is input to the controller. ACE is the power discrepancy between the assigned and actual output power which is the error signal E(t).

When the ACE is large, the proportional controller will be operated, whereas when the ACE is small, the integral controller will be operated. This controller can switch between proportional and integral controllers in terms of switching limits. The structure of the SDMPI controller is shown in Fig 2. The switching limit is given by $\boldsymbol{\varepsilon}$ a non-zero value. It is to be greater than the steady-state error obtained by the system with a proportional controller.

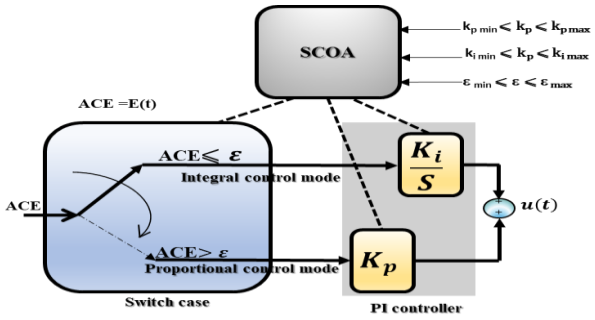

Fig. 2. SDMPI controller structure

$$U(t) = K_P E(t) \text{ for } |E(t)| = ACE > \varepsilon \quad (14)$$

$$U(t) = (K_i/s) E(t) \text{ for } |E(t)| = ACE \leq \varepsilon \quad (15)$$

$$U(t) = (K_i/s^{\lambda}) E(t) \text{ for } |E(t)| = ACE \leq \varepsilon \quad (16)$$

5.4. Design of Proposed SDMFOPI Controller

The construction of the SDMFOPI controller and the SDMPI controller is similar where the FOPI discussed in the previous section is utilized in place of the PI controller in the SDMFOPI controller. Due to the accuracy of the FO controller, which has a fractional operator that ranges from 0 to 1, it is preferred over the PI controller. İt is well known from the before discussed section that a switch in a dual-mode scheme of the controller allows one of two controllers to be connected to the feedback loop at the same time. Fig. 3 depicts the structure and working of the SDMFOPI controller. The first controller employs a linear feedback law, whereas the second operates by switching between two states.

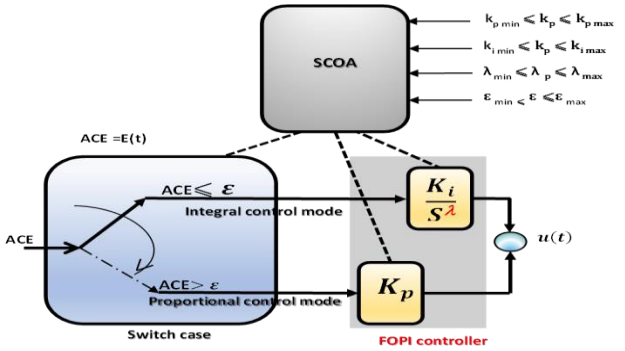

Fig. 3. SDMFOPI controller structure

According to the eqn (14), (16) when the input signal E(t) (error signal) ACE is greater than the switching limit (ACE>ε) the fractional order proportional controller mode is operated. Similar to this, a fractional order integral controller is used when ACE is below the switching limit (ACE≤ε). It is understandable from the definition above that the only operational difference between SDMFOPI and SDMPI is the presence of a FOPI controller in place of a PI controller. As a result, whereas the SDMPI controller switches between proportional and integral controllers whereas SDMFOPI controller switches between fractional order PI controller.In this work, four types of controllers were discussed for the considered hybrid system to mitigate the load frequency control problem.The controller chosen is based on their freedom of tuning and their accuracy .As in Table 1 the conventional PI controller has two tunable parameters of K_p and the K_i and SDMPI controller has three tunable parameters of K_p, K_i and switching limit ε.whereas the FOPI controller also has three tunable parameters of K_p, K_i and fractional operator λ. The proposed SDMFOPI controller has four tunable parameters of K_p ,K_i, fractional operator λ and switching limit ε .Thus the proposed SDMFOPI controller gives more freedom in tuning the system parameters .Along with dual mode scheme the FOPI controller in the controller structure of the proposed controller improves its accuracy thereby improving the system performance.

Table 1. Tunable parameters of the controller

Tunable parameters	PI	SDMPI	SFOPI	SDMFOPI
K_p	✓	✓	✓	✓
K_i	✓	✓	✓	✓
λ			✓	✓
ε		✓		✓

6. Problem Formulation and SCO Algorithm

This section covers problem formulation and the SCO algorithm.

6.1. Problem Formulation

The values of controller gains that have been optimized are linked to the objective function's minimal value. The LFC problem's main purpose is to lower the frequency deviation by minimizing the error. The parameter that decides the system's sensitivity and accuracy is termed the performance index(J). It is a function of various system parameters. In designing the controlle, various parameters are to be considered, as to minimize overshoot, undershoot, and

settling time. By considering only this performance index, since it is a function of various parameters it will be easy for computation. ISE (Integral Square Error), ITAE (Integral Time Absolute Error), IAE (Integral Absolute Error), etc. are some performance indexes commonly used. In this study, ISE was used as the objective function since they had the least degree of overshoot.

Min J_{ISE}

$$J_{ISE} = \int_0^{t_{max}} \sum_{i=1}^{n} (\Delta F^2_j + \Delta P^2_{j\_tieline}).dt \quad (17)$$

$$\begin{Bmatrix} K_{pmin} \le K_p \le K_{pmax} \\ K_{imin} \le K_i \le K_{imax} \\ \lambda_{min} \le \lambda_i \le \lambda_{max} \\ \varepsilon_{min} \le \varepsilon_i \le \varepsilon_{max} \end{Bmatrix} \quad (18)$$

Where in (17), ΔFj is Frequency change and ΔPj_tieline is tie-line power change in the jth area for small load change. And equation (18) is constraints and can be defined using the minimum and maximum values of the variables, respectively. The sum of the square of the change in frequency(ΔFj) in each area along with (ΔPj_tieline) is continuously integrated by ISE.

6.2. Sine Cosine Optimization Algorithm

In 2016, Syedali Mirjalili proposed the new population-based metaheuristic sine cosine optimization algorithm (SCOA) [31]. The name of the algorithm comes from the inclusion of sine and cosine in the method's formulation. This SCOA is utilized in different filed of research [32-34]. Due to its efficient working and simple procedural steps and fast convergence over other algorithms. SCOA generates random solutions in a search space, much like any other algorithm. This SCOA optimization process is typically separated into two phases: exploration and exploitation. An optimization method finds the search space by merging random solutions in a set of solutions with a high rate of unpredictability. This is referred to as the exploratory phase However, there are incremental modifications in the random solutions in the next phase, exploitation, and random variations are far smaller than in the exploration phase. It offers several advantages, including being versatile, adaptable, easy to integrate with other techniques, and capable of managing challenging optimization, among others.

$$X\,n^{i+1} = X^i_n + r1*\cos(r2) *|r3P^i_n \text{ —— } X^i_n| \quad (19)$$

$$X\,n^{i+1} = X^i_n + r1*\sin(r2) *|r3\ P^i_n \text{ —— } X^i_n| \quad (20)$$

$$X\,n^{i+1} = \{ X^i_n + r1*\cos(r2) *|r3\ P^i_n \text{ —— } X^i_n \mid r4 < 0.5$$

$$X^i_n + r1*\sin(r2)*|r3P^i_n \text{ —— } X^i_n| r4 \ge 0.5\} \quad (21)$$

The following lines show the pseudo-code for the SCO algorithm.

Initialize No. of solution

Evaluate the objective function for each solution

Update the obtained best solution

Update the r2, r2, r3, and r4

Update the position of the solution

While reaching maximum iteration

End

Where equations (20)-(21) represent the updated equations of the algorithm. I and n denote iteration and dimension, r1, r2, r3, and r4 represent random numbers [35], Xin is the position of the current solution, and Pin is the position of the best solution. The number of search agents is set to 20 throughout this research work, while the number of iterations is set at 50. The procedural process flow of the algorithm is represented in Fig. 4. At first, the number of random solutions and then bounds for the gains, switching limits, and maximum iterations are initialized.

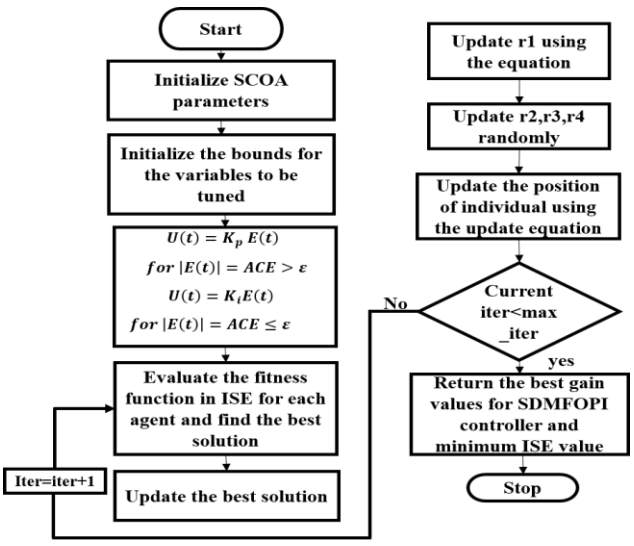

Fig. 4. Flow Chart of SCO algorithm

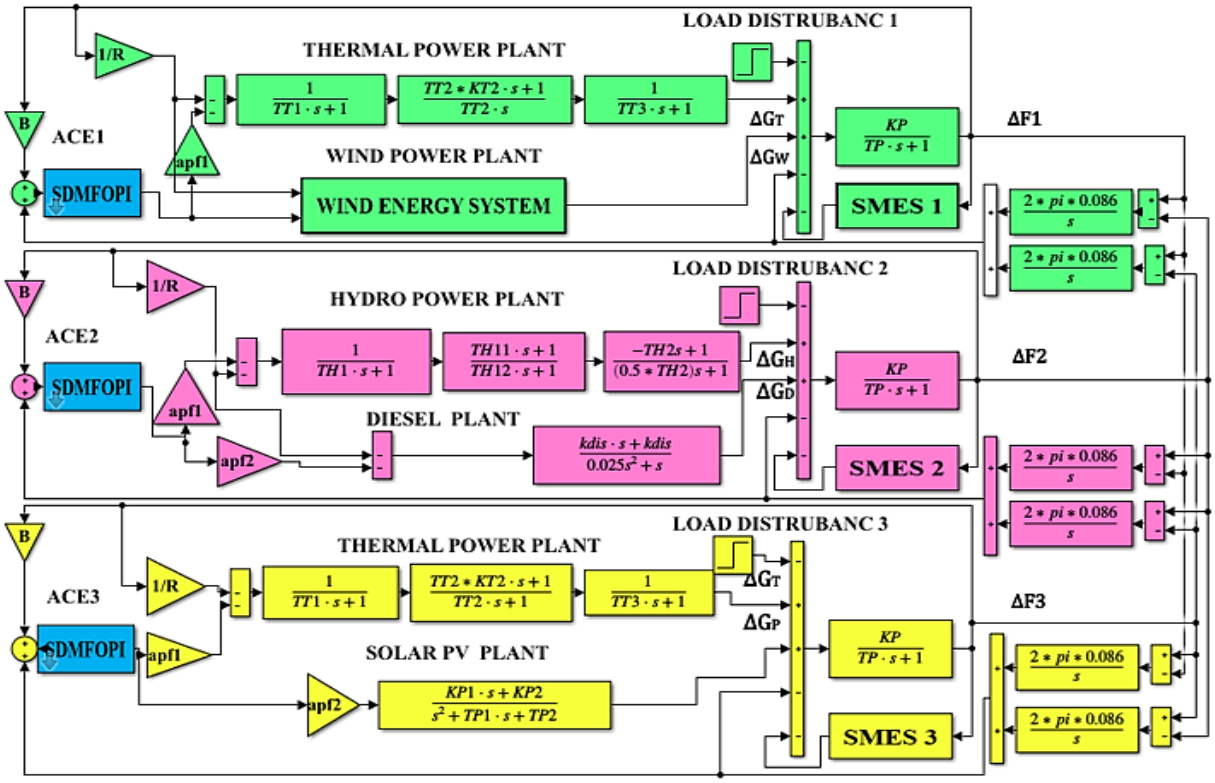

Fig. 5. Simulink diagram TAHPS with proposed SDMFOPI controller

And then the objective function is evaluated, the gains are tuned according to the ACE, and the best solution is obtained. Finally, random numbers are updated. Up to the maximum iterations, this process is repetitive. Thus, the SCOA is employed in minimizing the objective function in the ISE criterion and yielding the optimal gain values under different operating conditions.

7. Simulation Results and Discussions

In this research work, the SDMFOPI controller was designed and tested for TAHPS in the MATLAB platform. The transfer function model simulated is depicted in Fig. 5. The obtained results with the proposed controller are compared with other such controllers as the conventional PI controller, the SDMPI controller, and the SFOPI controller for 1% SLP. Table 2 shows the performance index obtained for different controllers for TAHPS. Figs. 6-11 show the corresponding frequency change in each area and the tie-lines and Table 3 shows the numerical results of undershoot, settling time, and undershoot. The proposed controller achieves the lowest errors. To verify that, different cases are discussed along with sensitivity analysis.

Table 2. The performance index obtained for different controllers for TAHPS

Controller type	PI	SDMPI	SFOPI	SDMFOPI
Performance index	0.00283	0.005639	0.002769	**0.002539**

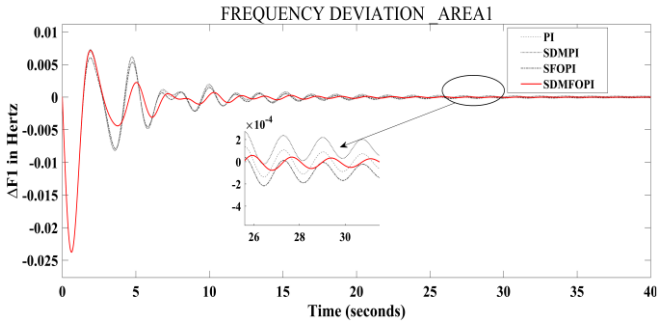

Fig. 6. Frequency change in area1

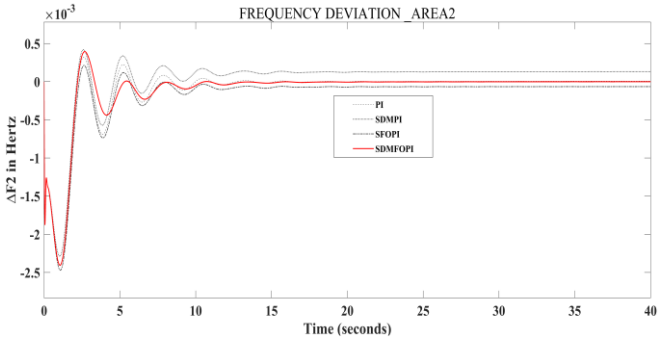

Fig. 7. Frequency change in area2

Table 3. Numerical results of TAHPS with 1% SLP

Parameter	ΔF and ΔT_{13}	PI	SDMPI	SFOPI	SDMFOPI
Undershoot	ΔF1	0.0237	0.0237	0.0237	0.0233
	ΔF2	0.0024	0.0024	0.0024	0.0022
	ΔF3	0.0281	0.0279	0.0284	0.0275
	ΔT_{13}	0.0080	0.0078	0.0087	0.0076
Overshoot	ΔF1	0.0068	0.0070	0.0060	0.0058
	ΔF2	0.0003	0.0004	0.0001	0.00009
	ΔF3	0.0175	0.0175	0.0172	0.0160
	ΔT_{13}	0.01109	0.01109	0.01109	0.01105
Settling time in (secs)	ΔF1	16.230	16.248	16.207	11.625
	ΔF2	11.870	16.248	9.7902	10.00
	ΔF3	13.760	13.807	13.667	11.936
	ΔT_{13}	25.719	27.363	25.697	20.035

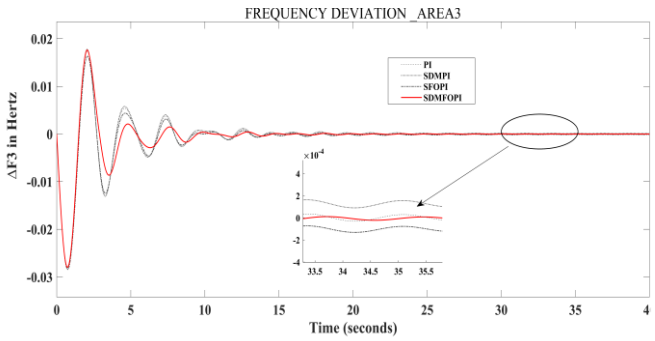

Fig. 8. Frequency change in Tie-line1

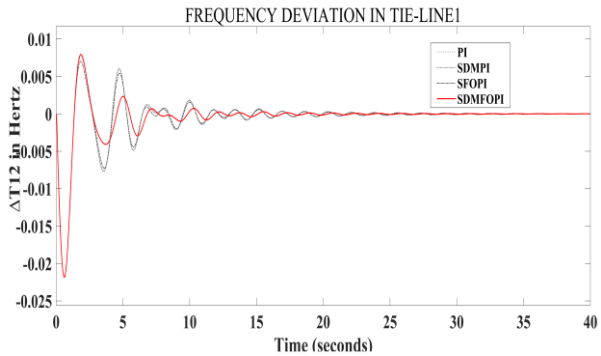

Fig. 9. Frequency change in Tie-line2

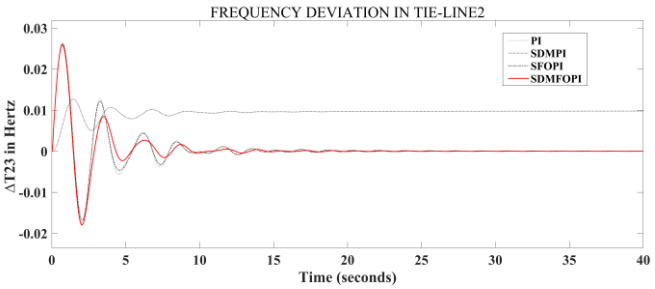

Fig. 10. Frequency change in Tie-line2

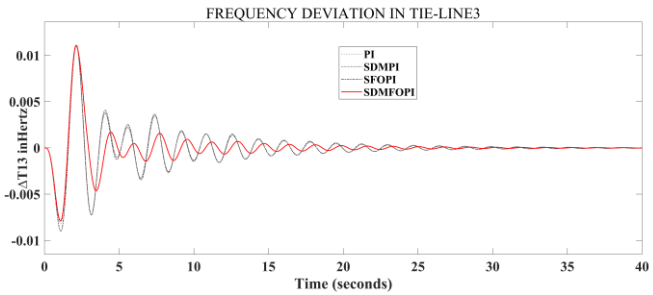

Fig. 11. Frequency change in Tie-line3

7.1. Controllerperformance analysis

7.1.1. Case1:TAHPS With Solar Dynamics and Varying Load

It is essential to investigate the proposed SDMFOPI under solar dynamics and load disturbances. The solar radiation in the range of [0.01, 0.02] p.u for 40 secs is applied to the TAHPS as in Fig. 5 and the corresponding output is in Fig. 12. And the next random varying load disturbance is applied to all areas at the same time. The corresponding frequency changes are obtained for all areas. Here, area1 output for varying load disturbance is shown in Fig. 13. The obtained performance requirements for the TAHPS achieved the best via the suggested SDMFOPI controller in both conditions of the presence of solar dynamics and varying load.

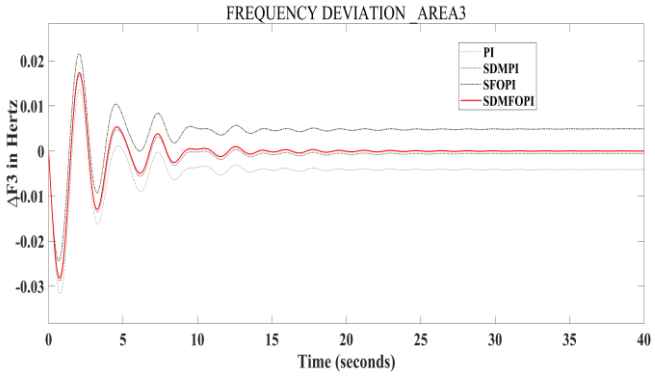

Fig. 12. Frequency change in area 3 by incorporating solar dynamics

Table 4. Numerical results of TAHPS for case 2

		ΔF1	ΔF2	ΔF3	ΔT_{13}
PI	**Base case**	-0.006808	0.007613	0.01209	0.01889
	For 2% of SLP	-0.01376	0.01523	0.02426	0.03801
	Difference	**0.006952**	**0.007617**	**0.01217**	**0.02612**
SDMPI	**Base case**	0.0001145	0.0001316	0.0001371	0.02262
	For 2% of SLP	0.0002282	0.0002633	0.0002748	0.04665
	Difference	**0.0001137**	**0.0001317**	**0.0001377**	**0.02403**
SFOPI	**Base case**	-0.09198	-0.06489	-0.00908	0.001148
	For 2% of SLP	-0.0001841	-0.0001298	-0.0001816	0. 002516
	Difference	**0.09179**	**0.06476**	**0.090628**	**0.01368**
SDMFOPI	**Base case**	0.000423	-0.0005274	-0.000921	-0.01344
	For 2% of SLP	-0.000563	-0.0009541	-0.008945	-0.00331
	Difference	**0.000986**	**0.0004267**	**0.008024**	**0.010125**

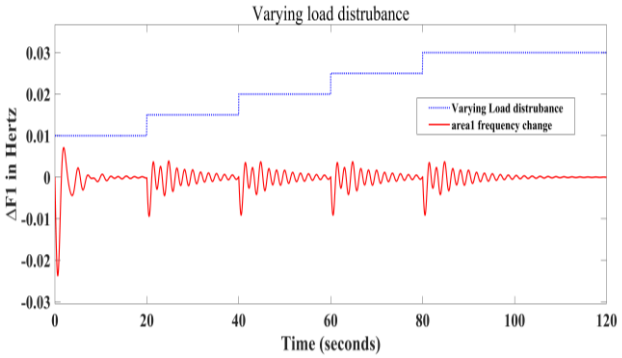

Fig. 13. Frequency change in area 1 for varying load

7.1.2. Case 2: Controller performance under different operating conditions

Also, simulation is carried out for 1% SLP (base case) and 2% SLP, and corresponding results are given in Table 4. From the table, it is clear that the difference between loading conditions is very small for the SDMFOPI controller when compared with other controllers. Therefore, for TAHPS under load variations, the suggested SDMFOPI for LFC is valid, superior, efficient, and capable of achieving the desired frequency and n tie-line power deviations.

7.1.3. Case 3: TAHPS With HVDC link

In this case, the HVDC line along with tie lines is employed in TAHPS for a range of reasons, including high current carrying capacity, simplicity, simple construction, fewer stability difficulties, and power regulation. The transfer function of the HVDC line is given in (11). Fig.14 shows the results for the corresponding case. It is clear from the result that integrating HVDC along the AC tie line will considerably improve the system performance significantly, with very little to no overshoot and undershoot and very small steady-state error.

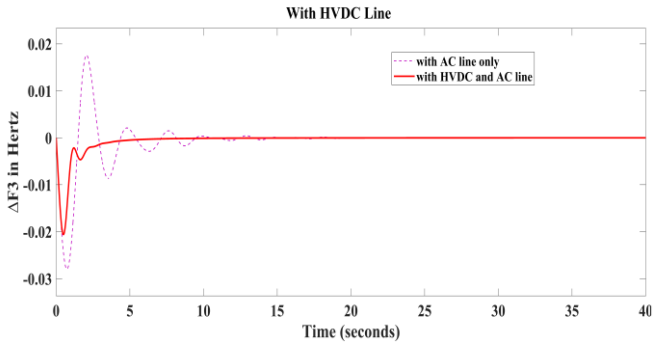

Fig. 14. Frequency change in area 3 with both HVDC and AC tie-lines

Table 5. Different scenarios considered

Scenario1		**Scenario2**		**Scenario3**		**Scenario4**			**Scenario5**		
Variation (%)	**+25**	**-25**	**+10**	**+25**	**-10**	**+10**	**+25**	**-10**	**+25**	**-25**	**+10**
Parameter	**T_{T3}**	**K_{P1}**	**K_{W2}**	**K_{DIS}**	**K_{T2}**	**R**	**T_{H12}**	**T_{T1}**	**B**	**T_{P1}**	**T_{W2}**
Nominal value	0.3	18	1.4	16.5	0.33	2.4	10	0.08	0.425	100	0.041
New Value	0.375	13.5	1.54	20.625	0.297	2.64	12.5	0.072	0.531	75	0.045

7.2. Sensitivity Analysis

To confirm the proposed controller's superiority and validity the parameters of the TAHPS are varied. It is subjected to a sensitivity test by changing some parameters. Table 5 depicts five possible scenarios, each of which has a different value variation. The matching output of each scenario is depicted in Figs. 15-19. It is obvious from the output that the suggested SDMFOPI controller is adaptable to varying system characteristics.

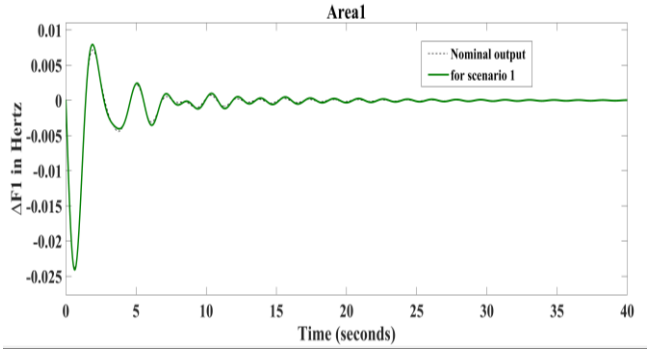

Fig. 15. Frequency change in area 1 for scenario 1

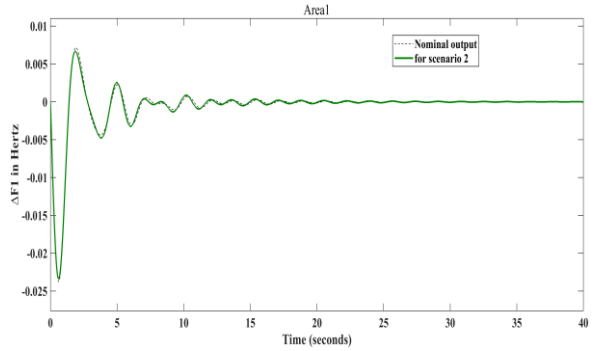

Fig. 16. Frequency change in area 1 for scenario 2

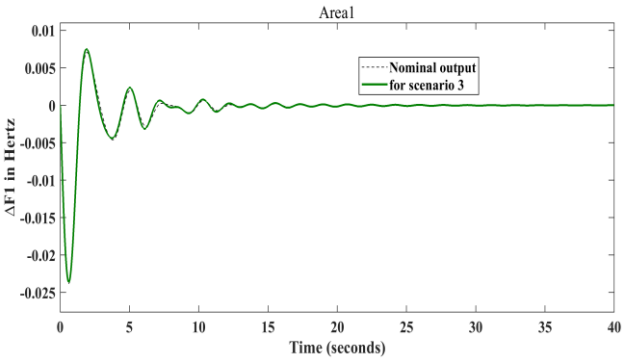

Fig. 17. Frequency change in area 1 for scenario 3

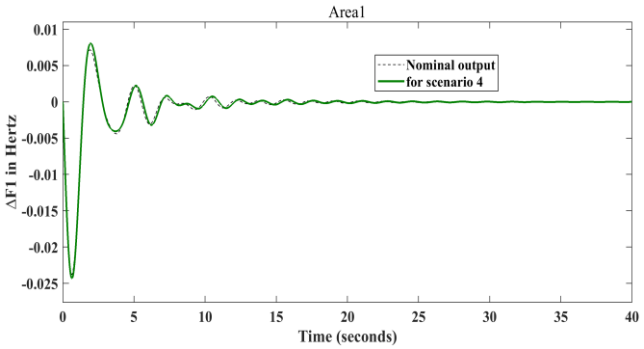

Fig. 18. Frequency change in area 1 for scenario 4

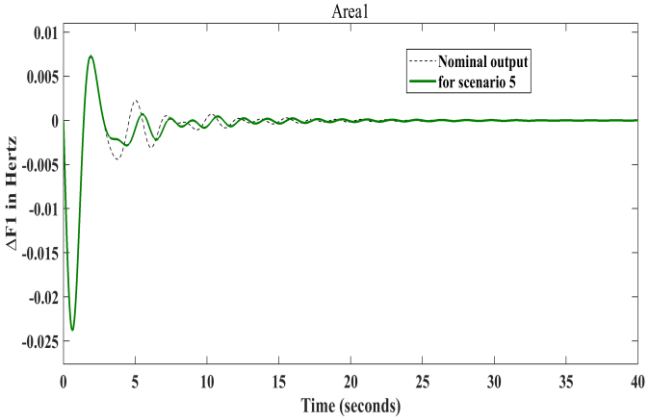

Fig. 19. Frequency change in area 1 for scenario 5

8. Conclusion

In this proposed research work, an SDMFOPI controller is designed and successfully implemented to mitigate the LFC problem of TAHPS. A sine cosine optimization algorithm is utilized for tuning the gains of the controller. Alternative controllers of PI, SDMPI, and SFOPI controllers are also built and compared with the proposed controller for 1% of step load change. The authors conclude with the following points.

- In the Three area hybrid power system, the proposed Sine cosine optimization-based dual-mode fractional order controller is successfully implemented and it achieved the minimum best integral square error (ISE) of 0.0025 comparing other controllers with less settling time.
- By implementing the proposed SDMFOPI controller the system achieved fewer undershoot overshoot frequencies in all the areas and the tie-line.
- Different cases of systems with solar dynamics, a system with varying load disturbance, and a system with both HVDC and AC tie-line are discussed. From this performance analysis, the superiority of the proposed controller is verified.
- In the three-area hybrid power system (TAHPS), sensitivity analysis is carried out in different scenarios with varying system parameters. And the result proved the proposed controller's robustness.

Finally, from the comparison of results, it is evident that the SDMFOPI controller is more efficient in settling time, overshoot, and undershoot aspects in different areas and tie-lines of the TAHPS. In addition, sensitivity analysis and performance analysis demonstrated the robustness and superiority of the proposed controller.

Acknowledgements

The authors thank the Department of science and technology (DST), New Delhi for having provided the necessary facilities through the FIST-level l program in the Energy Conversion Lab attached to the Department of Electrical Engineering at Annamalai University, to carry out the work relating to the area under study.

Appendix

Thermal plant: T_{T1}=0.08s; T_{T2}=10s; KT2=0.33 Hz/puMW; TT3 =0.3s
Wind plant: K_{W1}=1.25; T_{W1}=0.6; K_{W2}=1.4; T_{W2}=0.041s
Power system: KPS= 120 Hz/pu MW; TPS=20 s; B=0.425 Hz/pu MW;
R=2.4 puMW/Hz; apf1=0.65 apf2=0.35
Hydro plant:T_{H1}=48.7 s; T_{H11}=0.513 s; T_{H12}=10s; T_{H2}=1s
Diesel plant: K_{DIS}=16.50
Solar plant: K_{P1}=-18;¬T_{P2}=100s; K_{P2}=900; T_{P2}=50 s.
SMESs.
SMES1: T_{11} =0.1011; T_{12}= 0.1288; T_{13}=0.3849; T_{14} =0.2098; K_{SMES} =0.4901; T_{SMES1} =0.6189
SMES2: T_{21}=0.4772; T_{22}= 0.9078; T_{23}= 0.6535; T_{24}=0.1127; K_{SMES} =0.1000; T_{SMES} =0.6488
SMES3: T_{31}=0.1538; T_{32}= 0.2180; T_{33}=0.8086; T_{34} =0.1192; K_{SMES} =0.9210; T_{SMES} =0.2407.

References

[1] Y. Mi, Y. Xu, Z. Lang, X. Yang, X. Ge, Y. Fu, and C. Jin, "The frequency-voltage stability control for isolated wind-diesel hybrid power system," *Electric Power Systems Research*, DOI: 10.1016/j.epsr.2020.106984, Vol. 192, March 2021.

[2] Z. A. Thoker and S. A. Lone, "Voltage and frequency control of wind-diesel power system through adaptive sliding mode control of superconducting magnetic energy storage",*Wind Engineering*, DOI: 10.1177/0309524X20949526, Vol. 45, No. 5, pp. 1057–1071, August 2021.

[3] J. Liu, Q. Yao, and Y. Hu, "Model predictive control for load frequency of hybrid power system with wind power and thermal power," *Energy*, DOI: 10.1016/j.energy.2019.01.071, Vol. 172, pp. 555–565, April 2019.

[4] T. Mahto, H. Malik, and V. Mukherjee, "Fractional order control and simulation of wind-biomass isolated hybrid power system using particle swarm optimization," *Advances in Intelligent Systems and Computing*, *Springer Verlag*, DOI:10.1007/978-981-13-1819-1_27 Vol. 698, pp. 277–287, January 2019.

[5] C. Ghenai and M. Bettayeb, "Grid-Tied Solar PV/Fuel Cell Hybrid Power System for University Building," *Energy Procedia*, DOI: 10.1016/j.egypro.2018.12.025 Vol. 159, pp. 96–103, February 2019.

[6] L. Khalil, K. Liaquat Bhatti, M. Arslan Iqbal Awan, M. Riaz, K. Khalil, and N. Alwaz, "Optimization and designing of hybrid power system using HOMER pro," *Materials Today: Proceedings*, DOI: 10.1016/j.matpr.2020.06.054, Vol. 47, pp. S110–S115, July 2020.

[7] S. B Mohod, V. R. Parihar, and S. D. Nimkar, "Hybrid Power System with Integration of Wind, Battery, and Solar PV System," *IEEE International Conference on Power, Control, Signals and Instrumentation Engineering (ICPCSI)*, pp. 2332-2337, September 2017.

[8] Y. R. Prajapati, V. N. Kamat, and J. Patel, "Load Frequency Control Under Restructured Power System Using Electrical Vehicle as Distributed Energy Source,"

Journal of The Institution of Engineers (India): Series B, DOI:10.1007/s40031-020-00458-5, Vol. 101, No. 4, pp. 379–387, August 2020.

[9] S.S. Pati, A. Behera and T.K. Panigrahi, "Automatic generation control of renewable energy based multi-area system with plug in electric vehicle", *International Journal of Renewable Energy Research (IJRER)*, DOI:10.20508/ijrer. v10i1.10217.g7837), Vol.10, No. 1, pp. 54-66, March 2020.

[10] S.S. Pati and S.K. Mishra, "Contribution of energy storage technologies in load frequency control-a review", *International Journal of Renewable Energy Research (IJRER)*, DOI:10.20508/ijrer. v10i2. 10729.g7954, Vol.10, No. 2, pp. 871-891, June 2020.

[11] H. Haes Alhelou, M. E. Hamedani-Golshan, R. Zamani, E. Heydarian-Forushani, and P. Siano, "Challenges and opportunities of load frequency control in conventional, Modern and future smart power systems: A comprehensive review," *Energies*, DOI:10.3390/en11102497, Vol. 11, No. 10, October 2018.

[12] J. Sharma, Y.V. Hote, and R. Prasad, "PID controller design for interval load frequency control system with communication time delay," *Control Engineering Practice*, DOI: 10.1016/j.conengprac.2019.05.016 Vol. 89, pp. 154–168, August 2019.

[13] D. Mohanty and S. Panda, Lecture Notes in Networks and Systems, 1st ed., Vol. 151, Springer Singapore,2021, pp. 117–128, 2021.

[14] A. Ghosh, K. Ray, M. Nurujjaman, and M. Jamshidi, "Voltage and frequency control in conventional and PV integrated power systems by a particle swarm optimized Ziegler–Nichols based PID controller," *SN Applied Sciences*, DOI:10.1007/s42452-021-04327-8, Vol. 3, No. 3, pp. 1-13, March 2021.

[15] S. Padhy and S. Panda, "Simplified grey wolf optimization algorithm tuned adaptive fuzzy PID controller for frequency regulation of interconnected power systems," *International Journal of Ambient Energy*, DOI:10.1080/01430750.2021.1874518, pp. 1–13, January 2021.

[16] A. Behera, T.K. Panigrahi, S.S. Pati, S. Ramasubbareddy and A.H Gandomi, "A hybrid evolutionary algorithm for stability analysis of 2-area multi-non-conventional system with communication delay and energy storage", *International Journal of Electrical Power and Energy Systems (IJEPES)*, Vol.130, pp.106823, September 2021.

[17] A. Behera, T. K Panigrahi, P. K Ray and A. K. Sahoo, "A novel cascaded PID controller for automatic generation control analysis with renewable sources", *IEEE/CAA Journal of Automatica Sinica*, Vol.6, No.6, pp. 1438-1451, DOI:10.1109/JAS.2019.1911666, September 2019.

[18] K. Thenmalar, "Fuzzy logic based load frequency control of power system," in *Materials Today: Proceedings*, DOI: 10.1016/j.matpr.2021.02.536, Vol. 45, No.9, pp. 8170–8175, January 2021.

[19] A.Behera, T.K.Panigrahi and A.K.Sahoo, "A FO-PID controlled automatic generation control of multi area power systems tuned by harmony search", *Recent Advances in Electrical and Electronic Engineering*, Vol.13, No.1, pp. 101-109 2020, February 2020.

[20] S. Bhongade and V.P. Paramar, "Automatic generation control of two-area ST-Thermal power system using jaya algorithm", *International Journal of Smart Grid*, Vol:2, No:2, pp. 99-110, June 2018.

[21] Y. Tominaga, M. Tanaka, H. Eto, Y. Mizuno, N. Matsui and F. Kurokawa, "Design optimization of renewable energy system using EMO", *IEEE International Conference on Smart Grid (icSmartGrid)*, pp. 258-263, December 2018.

[22] H. H. Ali, A. Fathy and A. M. Kassem, "Optimal model predictive control for LFC of multi-interconnected plants comprising renewable energy sources based on recent sooty terns approach," *Sustainable Energy Technologies and Assessments*, DOI: 10.1016/j.seta.2020, Vol. 42, pp. 100844, December 2020.

[23] R. K Sahu, T. S. Gorripotu and S. Panda, "Automatic generation control of multi-area power systems with diverse energy sources using teaching learning based optimization algorithm", *Engineering Science and Technology, an International Journal*, DOI: 10.1016/j.jestch.2015.07.011Vol.19, No.1, pp.113-134, March 2016.

[24] S. Kotra and M. K Mishra, "Energy management of hybrid microgrid with hybrid energy storage system", *IEEE International Conference on Renewable Energy Research and Applications (ICRERA)*, pp. 856-860, November 2015.

[25] T. Atasoy, H. E Akınç and Ö. Erçin, "An analysis on smart grid applications and grid integration of renewable energy systems in smart cities", *IEEE International conference on renewable energy research and applications (ICRERA)*, pp. 547-550, November 2015.

[26] S. Vadi, F B.Gürbüz, R. Bayindir and E. Hossain, "Design and Simulation of a Grid Connected Wind Turbine with Permanent Magnet Synchronous Generator", *IEEE 8th International Conference on Smart Grid (icSmartGrid),* pp. 169-175, June 2020.

[27] N. K. Jena and S. Sahoo, Lecture Notes in Networks and Systems,1st ed., Vol. 151, *Springer Singapore,*2021, pp. 277–288.

[28] D. Sharma and N.K Yadav, "LFOPI controller: a fractional order PI controller based load frequency control in two area multi-source interconnected power system", *Data Technologies and Applications,* DOI 10.1108/DTA-08-2019-0126, Vol. 54, No. 3, pp. 323-342, April 2020.

[29] M. R. Sathya and M. Mohamed Thameem Ansari, "Design of biogeography optimization based dual mode gain scheduling of fractional order PI load frequency controllers for multi source interconnected power systems," *International Journal of Electrical Power and Energy Systems*, DOI: 10.1016/j.ijepes.2016.04.006, Vol. 83, pp. 364–381, December 2016.

[30] S. Velusami and I.A. Chidambaram, "Decentralized biased dual mode controllers for load frequency control of interconnected power systems considering GDB and GRC non-linearities", *Energy Conversion and Management,* DOI: 10.1016/j.enconman.2006.11.003, Vol.48, pp.1691–1702, December 2006.

[31] S. Mirjalili, "SCA: A Sine Cosine Algorithm for solving optimization problems," *Knowledge-Based Systems*, DOI:10.1109/SPC.2018.8703982, Vol. 96, pp. 120–133, March 2016.

[32] S. Kaur and S. Prashar, A novel sine cosine algorithm for the solution of unit commitment problem", *International Journal of Science, Engineering and Technology Research,* Vol:5, No.12, pp.3298–3310.

[33] Y Hao, L Song, L Cui and H Wang," A three-dimensional geometric features-based SCA algorithm for compound faults diagnosis", *Measuremen*t, DOI: 10.1016/j.measurement.2018.10.098, Vol:134, pp. 480-91, February 2019.

[34] N. Patel and K. Bhattacharjee," A comparative study of economic load dispatch using sine cosine algorithm", *Transactions on Computer Science & Engineering and ElectricalEngineering(D),*DOI:10.24200/SCI.2018.50635.1796 2020, Vol.27, No.3, pp. 1467-1480, June 2020.

[35] L. Abualigah and A. Diabat, "Advances in sine cosine algorithm: A comprehensive survey", *Artificial Intelligence Review*, DOI:10.1007/s10462-020-09909-3, Vol.54, No.4, pp. 2567-608, Apr 2021.